ANTIOXIDANTS & REDOX SIGNALING
Volume 14, Number 11, 2011

DOI: 10.1089/ars.2010.3321

ORIGINAL RESEARCH COMMUNICATION

Antiatherogenic Effect of Bisvanillyl-Hydralazone, a New Hydralazine Derivative with Antioxidant, Carbonyl Scavenger, and Antiapoptotic Properties

Benaissa Bouguerne,[1–3] Nadji Belkheiri,[2,3] Florence Bedos-Belval,[2,3] Cécile Vindis,[1,3] Koji Uchida,[4] Hubert Duran,[2,3] Marie-Hélène Grazide,[1,3] Michel Baltas,[2,3] Robert Salvayre,[1,3] and Anne Nègre-Salvayre[1,3]

Abstract

Reactive oxygen species (ROS) generated within the vascular wall trigger low-density lipoprotein (LDL) oxidation, lipid peroxidation, and carbonyl stress that are involved in atherogenesis. We recently reported that the antihypertensive drug, hydralazine, exhibits carbonyl scavenger and antiatherogenic properties, but only moderate antioxidant activity, so that high concentrations are required for inhibiting LDL oxidation. We aimed to develop agents sharing both antioxidant and carbonyl scavenger properties. We have synthesized a new hydralazine derivative, the bisvanillyl-hydralazone (BVH). BVH strongly inhibited LDL oxidation induced by copper and by human endothelial cells (HMEC-1), and prevented the formation of macrophagic foam cells. BVH reduced both the extracellular generation of ROS (superoxide anion and hydrogen peroxide) induced by oxidized LDL (oxLDL), as well as intracellular oxidative stress and proteasome activation, NFkappaB activation, and oxLDL-mediated proinflammatory signaling. In parallel, BVH prevented the carbonyl stress induced by oxLDL on cellular proteins, and blocked the apoptotic cascade as assessed by the inhibition of Bid cleavage, cytochrome C release, and DEVDase activation. Lastly, BVH prevented atherogenesis and carbonyl stress in apoE$^{-/-}$ mice. In conclusion, BVH is the prototype of a new class of antioxidant and carbonyl scavenger agents designed for new therapeutical approaches in atherosclerosis. *Antioxid. Redox Signal*. 14, 2093–2106.

Introduction

Oxidative stress plays a major role in atherogenesis and cardiovascular diseases (50), *via* its implication in the oxidative modifications of low-density lipoproteins (LDLs), that render them highly atherogenic (4, 7, 25, 54, 64). Oxidized LDL (oxLDL) are metabolically deviated toward macrophagic cells and taken-up *via* the scavenger receptor system, leading to the formation of foam cells that accumulate as fatty streaks in the arterial intima (43, 54, 55). Early lesions may be complicated by chronic inflammatory processes and local remodeling of the arterial wall, leading finally to more complex atherosclerotic plaques (33). Besides, oxLDLs exert various biological properties (including inflammation, cell proliferation, migration, growth arrest, and apoptosis) that play a role in the formation of complicated lesions, and in plaque erosion and rupture (31, 39, 44, 47, 48). These responses depend on the local concentration of oxLDLs, and on their content in lipid peroxidation products oxidized phospholipids, oxysterols (22, 30), and lipid peroxidation-derived aldehydes (4-hydroxynonenal [4-HNE], malondialdehyde [MDA], and acrolein) (13, 14, 59). These aldehydes react with free amino groups and thiol residues of proteins, thereby forming protein adducts ("carbonyl stress"), which modify and alter the function of circulating (*e.g.,* LDL) and cellular proteins (14, 40). Carbonyl stress occurs as a downstream consequence of oxidative stress, and it is inhibited when blocking lipid oxidation by antioxidants (52, 40). However, antioxidants fail to neutralize carbonyl stress, once adducts are formed on proteins (40, 42). Carbonyl stress is involved in cell growth arrest, inhibition of cell migration, inflammation, and (at a lesser extent) apoptosis, and is thought to contribute to the progression of atherosclerosis (40, 42).

The ability of antioxidants to reduce the coronary risk in humans is largely debated. The antiatherogenic effect of antioxidants has been extensively studied through *in vivo* preclinical studies on animal models for atherosclerosis and in

[1]Biochimie, INSERM U858, Team "Atherosclerosis," Toulouse, France.
[2]CNRS, Laboratoire de Synthèse et Physico-Chimie de Molecules d'Intérêt Biologique, Toulouse, France.
[3]Université Paul Sabatier, Toulouse Cedex, France.
[4]Laboratory of Food and Biodynamics, Graduate School of Bioagricultural Sciences, Nagoya University, Nagoya, Japan.

human trials (3, 5, 15, 23, 57, 63). Most antioxidants are highly efficient in preventing atherosclerosis development in animals (which mainly allow to investigate the first steps in atherogenesis, *i.e.,* foam cell formation), but fail to prevent the late athero-thrombotic complications of atherosclerosis and the subsequent cardiovascular events in human trials (3, 23, 63). The low apparent benefit of antioxidant therapy does not question the implication of oxidative stress and LDL oxidation in atherogenesis, as it may result from diverse mechanisms, such as difficulties in delivering effective *in situ* antioxidant therapy, including a lack of antioxidant availability, or a lack of effect on reactive oxygen species (ROS) involved *in vivo* in LDL oxidation and inflammatory signaling. Inhibiting carbonyl stress (which is a consequence of oxidative stress) may represent a new therapeutic strategy for patients, but so far, it is not known if the use of carbonyl scavengers could be beneficial or not on the late steps of atherosclerosis (40, 42). Most carbonyl scavengers usually exhibit poor antioxidant activity and inhibit neither LDL oxidation nor the generation of toxic lipid oxidation products (oxysterols and oxidized phospholipids), which are involved in the inflammatory and apoptotic events characterizing atherosclerosis progression (40). Hydrazine derivatives, such as the antihypertensive drug hydralazine, exhibit potent carbonyl scavenger efficiency associated with anti-atherogenic properties in apoE$^{-/-}$ mice, but present poor or moderate antioxidant properties, so that high concentrations (50–100 μM) are required for inhibiting cell-mediated LDL oxidation (16). Theoretically, agents sharing both antioxidant and carbonyl scavenger activities should inhibit each step of atherosclerosis progression, including LDL oxidation, oxidative stress, and carbonyl stress as well, and their consequences in the evolution toward advanced lesions.

We have designed and synthesized a hydralazine derivative, the bisvanillyl-hydralazone (BVH), and we have characterized its antioxidant, carbonyl scavenger, and antiatherogenic properties, more precisely its ability to (i) block oxidative stress, LDL oxidation, carbonyl stress, and foam cell formation, (ii) inhibit the inflammatory signaling of oxLDL, (iii) neutralize the apoptotic effect of oxLDL in cultured vascular cells, and (iv) slow down or inhibit the formation of atherosclerotic lesions in apoE$^{-/-}$ mice.

Materials and Methods

Chemicals

Antibodies directed against MCP-1, Bid, gp91^{phox}, and cytochrome C were from Santa Cruz (Tebu-Bio SA). Anti phospho-NF-κB was from Cell Signaling. AntiCD3 and anti α-actin antibodies were from R&D System. Anti 4-HNE antibody was prepared as reported (58). Acrylamide-4X/bisacrylamide-2$\times$solutions were from Euromedex; SYTO-13, 6-carboxy-2′,7′-dichlorodihydrofluorescein diacetate, di (acetoxymethyl ester) (H_2DCFDA-AM), dihydroethidium (DHE), and propidium iodide were from Molecular Probes (InVitrogen); cell culture reagents and other reagents were from WWR or Sigma.

Synthesis

Organic solvents were purified as described (41) or were purchased from Aldrich Chemie. Melting points (mp) were obtained on a Buchi apparatus and are uncorrected. Infrared (IR) spectra were recorded on a Perkin-Elmer 1725 IR spectrophotometer and the data are reported in inverse centimeters. UV spectra were recorded on a Perkin-Elmer lambda 17 UV-vis spectrophotometer. Proton nuclear magnetic resonance (^{1}H NMR) spectra were obtained with a Bruker AC-300 MHz spectrometer. Chemical shifts were reported in parts per million (ppm) and signals are given as follows: s, singlet; d, doublet; t, triplet; m, multiplet. Mass spectra were recorded on an R 10-10 C Nermag (70 eV) quadripolar spectrometer using desorption chemical ionization or electrospray techniques.

Bisvanilline 2 synthesis. To vanillin (10.64 g, 70 mmol) in 700 ml of water was added $FeSO_4$ (0.4 g, 1.4 mmol) under stirring. After heating during 10 min at 50°C, $Na_2S_2O_8$ (8.93 g, 37.5 mmol) was added. The reaction mixture was stirring at 50°C for 5 days. The brown precipitate formed was filtered off. The solid was dissolved in NaOH (2 *M*) aqueous solution. HCl (2 *M*) aqueous solution was added. Brown solid formed was isolated by filtration (10 g, 95%). mp > 270°C. IR (KBr) ν cm^{-1}: 3186 (O-H), 1672 (C = O), 1587 (C = C arom.), 1454 (C = C arom.). ^{1}H NMR (DMSO, 300 MHz) δ ppm: 3.94 (s, 6H, OCH_3), 7.42 (s, 4H), 9.80 (s, 2H, CHO), 9.89 (s, 2H, OH). ^{13}C NMR (DMSO, 75 MHz) δ ppm: 56.50 (s, 2C, OCH_3), 109.70 (s, 2C), 125 (s, 2C), 128.23 (s, 2C), 128.62 (s, 2C), 148.60 (s, 2C), 150.90 (s, 2C), 191.60 (s, 2C, CHO). UV (EtOH/0.2% DMSO, 25 μM, 25°C): λ = 303 nm, ε = 14,300 mol^{-1}.L.cm^{-1}.MS (FAB, MNBA) m/z: 303.1 [M+H$^+$].

BVH synthesis. 5,5′-Bisvanilline (BV) **2** (0.2 g, 0.66 mmol) was suspended in absolute ethanol (26 ml). Hydralazine hydrochloride (0.26 g, 1.32 mmol) was added. The reaction mixture was refluxed for 6h30 and filtrated to give pure BVH (0.38 g, 87%) as a yellow solid. mp > 270°C; IR (KBr) ν cm^{-1}: 3423 (O-H), 1675 (C = N), 1617 (C = C arom.), 1594 (C = C arom.), 1473 (C = C arom.). ^{1}H NMR (DMSO, 300 MHz) δ ppm: 3.94 (s, 6H, OCH_3), 7.41 (d, 2H, ^{4}J = 1.8 Hz), 7.78 (d, 2H, ^{4}J = 1.8 Hz), 8.10 (m, 6H), 8.68 (s, 2H, HC = N); 8.95 (s, 2H); 9.03 (s, 2H); 9.20 (d, ^{3}J = 7.3 Hz, 2H); 9.29 (bs, 2H, OH); 14.31 (bs, 2H, HCl).^{13}C NMR (DMSO, 75 MHz) δ ppm: 56.55 (s, 2C, OCH_3), 109.70 (s, 2C, C_2), 119.35 (s, 2C, C_8), 123.91 (s, 2C), 124.26 (s, 2C), 125.12 (s, 2C), 125.38 (s, 2C), 126.61 (s, 2C), 128.25 (s, 2C),128.62 (s, 2C), 134.12 (s, 2C), 136.27 (s, 2C), 147.70 (s, 2C), 148.29 (s, 2C), 148.46 (s, 2C), 157.75 (s, 2C, HC = N). UV (EtOH/0.2% DMSO, 25 μM, 25°C): λ = 376 nm, ε = 34,750 mol^{-1}.L.cm^{-1}, λ = 296 nm, ε = 21,500 mol^{-1}.L.cm^{-1} MS (IC, NH_3, pos) m/z: 587.2 [M+H$^+$].

Cell culture

Human microvascular endothelial cells (HMEC-1) (CDC, Dr. Candal) were grown in MCDB131 culture medium supplemented with 10% heat inactivated fetal calf serum, 100 U/ml penicillin, and 100 μg/ml streptomycin. Raw 264.7 murine macrophages were obtained from ATCC and were grown in DMEM. Twenty-four hours before LDL incorporation, cells were starved in serum-free RPMI medium.

LDL isolation and oxidation

LDL from human pooled sera were prepared by ultracentrifugation, and dialyzed against phosphate-buffered saline (PBS) containing 100 μM EDTA, as previously indicated (62).

The mechanism by which BVH protects against LDL oxidation has been compared *in vitro* on LDL oxidation mediated by transition metal-dependent (copper) and -independent (AAPH) systems. Native LDLs (1 mg/ml) were incubated in the presence of BVH (5 μM), and either with freshly prepared AAPH [2,2′-azobis-(2-amidinopropane) hydrochloride] (at the indicated concentrations, 2 h at 37°C) (49), or with copper ($CuSO_4$ 5 μM, 4 h incubation at 37°C). LDL oxidation was evaluated by determining the thiobarbituric acid-reactive substance (TBARS) content (16). To evaluate cell-mediated LDL oxidation, HMEC-1 were seeded in 12-multiwell plates. The standard culture medium was removed and replaced by serum-free RPMI 1640 containing native LDLs (100 μg apoB/ml). BVH, hydralazine, and BV were solubilized in DMSO, and added to the culture medium at the indicated concentrations (and 0.1% DMSO final concentration), simultaneously with LDLs. After incubation (14 h at 37°C), the LDL-containing medium was recovered for determining the TBARS and protein carbonyl content (16, 26). For all the other experiments, LDLs were mildly oxidized by UV/copper (in the absence of drug), as previously described (62). Under standard conditions, UV/Cu-oxLDLs contained 71–104 nmol lipid hydroperoxide/mg apoB and 6.4–9.7 nmol TBARS/mg apoB.

Protein carbonyl content and foam cell formation

The protein carbonyl content was determined using DNPH, according to Ichihashi *et al.* (26). The formation of foam cells was evaluated on Raw 264.7 macrophages incubated for 14 h in serum-free RPMI containing UV-oxLDL (100 μg/ml) and the agents at the indicated concentrations. After 14 h incubation, the LDL-containing culture medium was removed, cells were fixed in 0.4% paraformaldehyde/PBS for 10 min, washed in PBS, and stained with oil Red O, or fluorometrically quantified by Nile Red, as described (16).

Extracellular and intracellular ROS determination

Extracellular superoxide anion ($O_2^{\cdot -}$) generation was measured as the superoxide dismutase (SOD)-inhibitable reduction of cytochrome C. HMEC-1 preincubated for 1 h with native LDL (100 μg/ml), $CuSO_4$ (1 μM), and the molecules tested at 5 μM), were incubated in 1 ml phenol red-free RPMI containing cytochrome C (20 μM) with or without SOD (100 mU/l), for 30 min. The reduction of cytochrome C specific of $O_2^{\cdot -}$ (*e.g.*, SOD inhibitable) was determined spectrophotometrically at 550 nm (difference in absorbance with or without SOD), according to McCord and Fridovich (35). Extracellular hydrogen peroxide (H_2O_2) generation was determined as horseradish peroxidase (HRP)-dependent quenching of scopoletin fluorescence according to Loschen *et al.* (32), modified as follows: cells were incubated at 37°C in 1 ml of PBS containing 5 μM scopoletin and 30 nM HRP, and the fluorescence of the medium was read after 0, 30, and 60 min (ex/em 358/448 nm).

Intracellular ROS generated in cells treated by oxLDL (200 μg/ml) and the tested agents (1–5 μM) were evaluated by measuring the oxidation of H_2DCFDA-AM (for hydroperoxides) and DHE (for $O_2^{\cdot -}$) (10, 18). The probes were added to the culture medium (5 μM final concentration) 30 min before the end of the experiment. At the end, the cells were washed three times in PBS, and the fluorescence of the cell homogenate was measured as reported (ex/em 495/520 nm for H_2DCFDA, and 518/605 nm for DHE, respectively) (18). The data are expressed as ratio of fluorescence/fluorescence of the unstimulated control (12).

Proteasome activation

The *in vitro* activity of 20S proteasome was determined according to Grune *et al.* (21). Cells were homogeneized in PBS containing 0.1% Triton X-100 and 0.5 mM dithiotreitol, and the enzymatic activity was measured. The assay mixture contained 50 μl of buffer (50 mM Tris-HCl pH 7.8, 20 mM KCl, 5 mM $MgCl_2$, and 0.1 mM DTT), 250 μM of sLLVY-MCA, and 50 μl of cell homogenates (30 μg protein). After 30 min incubation at 37°C, the reaction was stopped by adding 1 ml of 0.2 M glycine buffer pH 10 and the fluorescence of the liberated 7-amino-4 methylcoumarin was measured (exc/em 365/460 nm, respectively).

Monocyte adhesion assay and MCP1 release in the culture medium

Monocyte adhesion assay was performed according to Srinivasan *et al.* (51). Briefly, Raw 264.7 macrophages were labeled with Calcein AM (5 μM) for 10 min at 37°C, rinsed three times in PBS, and resuspended in PBS. Labeled fluorescent monocytes were added (100,000/well) to HMEC-1 either unstimulated or stimulated (at the indicated times) with oxLDL (200 μg/ml) in the presence or absence of the different agents (5 μM), for 30 min. At the end, the cells were carefully washed three times with PBS for removing unbound monocytes, and then lysed in water by sonication; the fluorescence of the cell lysate was immediately determined by fluorometry (ex/em 490/525). MCP-1 released by cells was measured by ELISA in the culture medium of control and LDL-stimulated HMEC-1, with or without the tested agents, according to the indications of the manufacturer (Pierce).

Evaluation of cytotoxicity, necrosis and apoptosis

Cytotoxicity was evaluated using the MTT (3-(4,5-dimethylthiazol-2-yl)-2,5-diphenyltetrazolium bromide) test. Necrosis and apoptosis were determined by counting the cells (inverted fluorescence microscope Fluovert FU; Leitz), after staining with 2 vital fluorescent dyes, 0.6 μM SYTO-13 (a permeant DNA intercalating green-colored probe) and 1.5 μM propidium iodide (a non permeant intercalating red probe) (16). DEVDase activity (caspase 3) was determined using the fluorogenic substrate Ac-DEVD-AMC (N-acetyl-Asp-Glu-Val-Asp-7-amino-4-methylcoumarin) (40 μM), on cell lysates from HMEC-1 stimulated with oxLDLs (200 μg/ml) and the agents, as reported (16). After 30 min incubation at 37°C, the released fluorescent product AMC (aminomethylcoumarin) was determined by fluorometry (ex/em 351/430 nm).

Western blot analysis

Cells extracts were subjected to SDS-PAGE and revealed using the indicated primary and secondary antibodies conjugated with horseradish peroxidase, and developed by ECL (Amersham). Same protocol was applied on aortas from $apoE^{-/-}$ mice (16).

Western blot was quantified using NIH ImageJ software (http://rsbweb.nih.gov/ij/index.html).

Animal studies

ApoE KO (apoE$^{-/-}$) mice were from Transgenic Alliance (IFFA Credo; Les Oncins). Three groups of 20 male mice (4 weeks old), housed under specific pathogen-free conditions, were fed a standard diet supplemented (or not) with BVH or hydralazine (10 mg/kg in drinking water), as reported in (16, 38). Mice were killed at age 20 weeks. Mouse experiments were approved by the Committee on Research Animal Care of Inserm U-858 Center. Plasma cholesterol, triglycerides, and glycemia were determined immediately after sacrifice (AU 2700 Biochemistry Analyzer Olympus, CHU Rangueil Toulouse).

Quantification and characterization of atherosclerotic lesions

The lesions were estimated as described by Bucciarelli *et al.* (6). Hearts were washed in PBX, frozen on a cryostatmount with OCT compound (Tissue-Tek), and stored at −80°C. Serial sections 10 μm thick of aortic sinus were stained with oil Red O, counterstained with hematoxylin-eosin, and analyzed for morphometric evaluation of the lesion size, using a computerized Biocom morphometry system. The mean lesion size in aortic sinus was expressed in $\mu m^2 \pm$ SEM.

Immunohistochemistry

Fixed frozen cryo-sections (10 μm thick) of aortic sinus from control and BVH-treated mice were incubated with the antibodies, anti-CD3 (lymphocytes), anti-α-actin (SMC), anti-4-HNE-adducts (lipid peroxidation), and anti-MCP1. After incubation with appropriate biotin-labeled antibody, sections were revealed using avidin–biotin horseradish peroxidase visualization system (Vectastain, ABC kit Elite; Vector Laboratories).

Statistical analysis

Data are given as mean ± SEM. Estimates of statistical significance were performed by analysis of variance (one-way ANOVA, Tukey test, SigmaStat software).

Results

We recently reported that hydralazine is an efficient carbonyl scavenger agent with potent antiatherogenic effect (45% of lesion reduction in apoE$^{-/-}$ mice treated by 10 mg/kg/day hydralazine in drinking water during 16 weeks) (16). However, hydralazine exhibits only mild antioxidant properties, and relatively high concentrations are required to prevent LDL oxidation and subsequent formation of foam cells that accumulate in early atherosclerotic lesions. We aimed to improve the antioxidant properties of hydralazine, without altering its carbonyl scavenger properties. For this purpose we designed and synthesized a hydralazine derivative, and we report its ability to prevent LDL oxidation and oxLDL cytotoxicity, and to delay the formation of atherosclerotic lesions in apoE$^{-/-}$ mice.

BVH synthesis

BV was obtained through oxidative coupling reaction of 2 vanilline moieties. The reaction conditions were optimized and the best results were obtained when performing the coupling reaction in the presence of sodium persulfate and catalytic amount iron sulfate in water at 50°C (Fig. 1). The reaction was followed by thin layer chromatography till completion after 5 days, affording after work up BV with an excellent yield (95%). BV was then allowed to react with two equivalents of hydralazine hydrochloride in refluxing ethanol for 6h30 affording pure chlorhydrated BVH as a precipitated solid which was filtered off (87% yield).

BVH copper chelating properties

Transition metals are strongly implicated in the reductive decomposition of lipid hydroperoxides, to give alkoxyl and lipid peroxyl radicals during the propagation step. As some polyphenolic compounds block the oxidation induced by transition metal ion-induced by chelating copper or iron ions (36), we evaluated whether this mechanism was implicated in the protective effect of BVH against LDL oxidation. To clarify the ability of BVH to react with cupric ion, its interaction was assessed by UV-vis spectroscopy. The wavelength spectra of the complex formed between BVH (25 μM) and increased concentration of copper (10–80 μM) revealed absorbance peaks at 296 and 376 nm related to BVH alone (Fig. 2A). The increase in Cu(II) concentration caused a linear decrease in the absorbance at 296 and 376 nm and a linear increase in

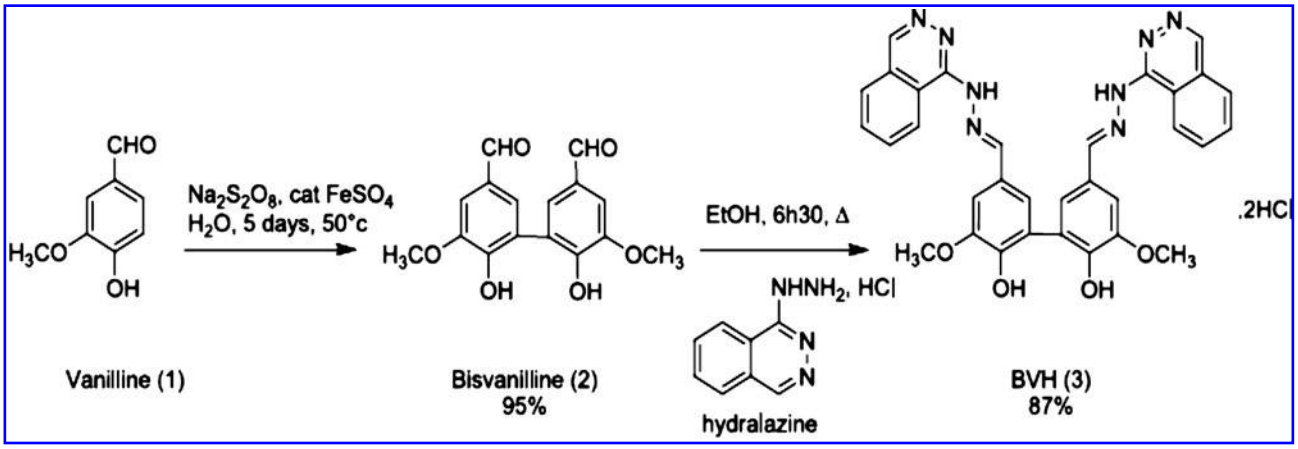

FIG. 1. Chemical structures of bisvanillyl-hydralazone (BVH), hydralazine (Hdz), and bisvanilline (BV), and scheme of BVH synthesis.

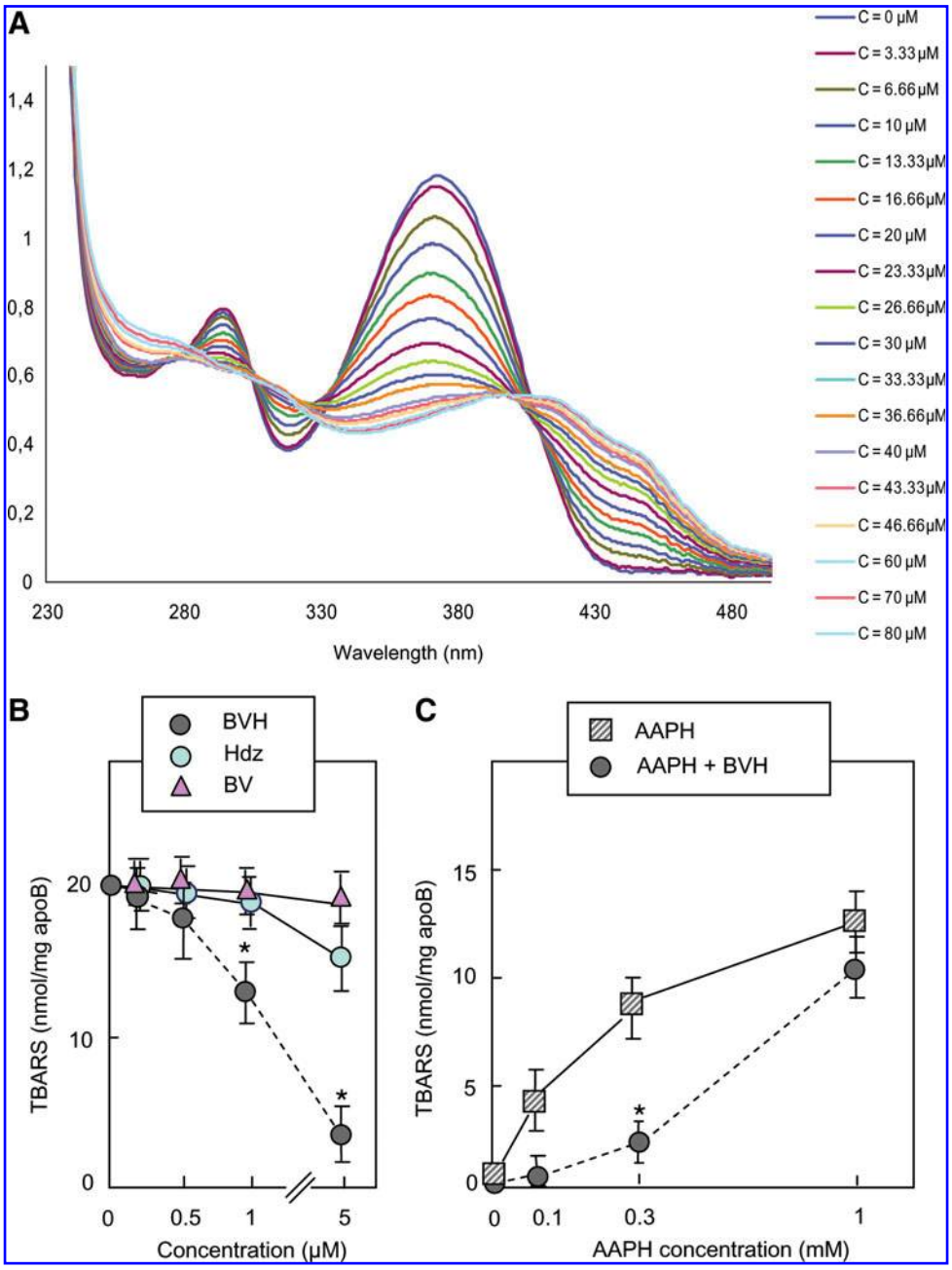

FIG. 2. BVH prevents copper-dependent low-density lipoprotein (LDL) oxidation. (A) Wavelength spectra of the complex formed between BVH (25 μM) and increasing copper concentrations (10–80 μM). The absorbance of the complex was measured at 296 and 376 nm related to BVH alone, and at 456 nm (absorbance of the complex). **(B)** Dose effect of BVH, Hdz, and BV on LDL oxidation (1 mg apoB/ml in phosphate-buffered saline [PBS]) induced by $CuSO_4$ (5 μM, 2 h incubation at 37°C). **(C)** Effect of BVH (5 μM) on LDL oxidation (1 mg/ml) incubated for 2 h at 37°C with variable concentrations of AAPH (2,2′-azobis-(2-amidino propane) hydrochloride) (0.1–1 mM as indicated). LDL oxidation was evaluated by the thiobarbituric acid-reactive substance (TBARS) content, as described in the Materials and Methods section, and the results were expressed as nmol TBARS/mg apoB in LDL oxidized in the absence of antioxidant. In **(B, C)**, the data are mean ± SEM of four separate experiments. *$p < 0.05$.

absorbance at 456 nm. Figure 2A also shows the formation of four isosbestic points at 274, 306, 330, and 415 nm in the presence of concentration of Cu(II) between 0 and 20 μM. The isosbestic points at 306, 330, and 415 nm shifted, respectively, to 299, 323, and 402 nm in the presence of 23.33 to 80 μM Cu(II). Altogether, these results indicate the formation of copper-BVH complexes.

BVH prevents metal- and AAPH-dependent LDL oxidation

The antioxidant properties of BVH were evaluated on its ability to block LDL oxidation induced *in vitro* by metal-dependent (copper) and -independent (AAPH) oxidation systems or by contact of LDL with HMEC-1. As shown on Figure 2B, low concentrations of BVH (1–5 μM) prevented copper-mediated LDL oxidation (monitored by TBARS formation), in contrast to hydralazine and BV, which had no (or only minor) effect at these concentrations. BVH efficiently inhibited LDL oxidation mediated by AAPH (100 and 300 μM), indicating that it also exhibits free radical scavenger properties in metal-independent oxidation systems (Fig. 2C). Likewise, BVH inhibited cell-mediated LDL oxidation and subsequent cytotoxicity, whereas hydralazine and BV had no effect (Fig. 3A, B).

Since cell-mediated LDL oxidation depends on the secretion of ROS in the extracellular medium, we evaluated the ability of BVH to reduce the level of extracellular ROS, namely, superoxide anion ($O_2^{\cdot -}$) and hydrogen peroxide (H_2O_2). BVH (1 and 5 μM) reduced the generation of $O_2^{\cdot -}$ and H_2O_2 (Fig. 3C, D), in agreement with its inhibitory effect on

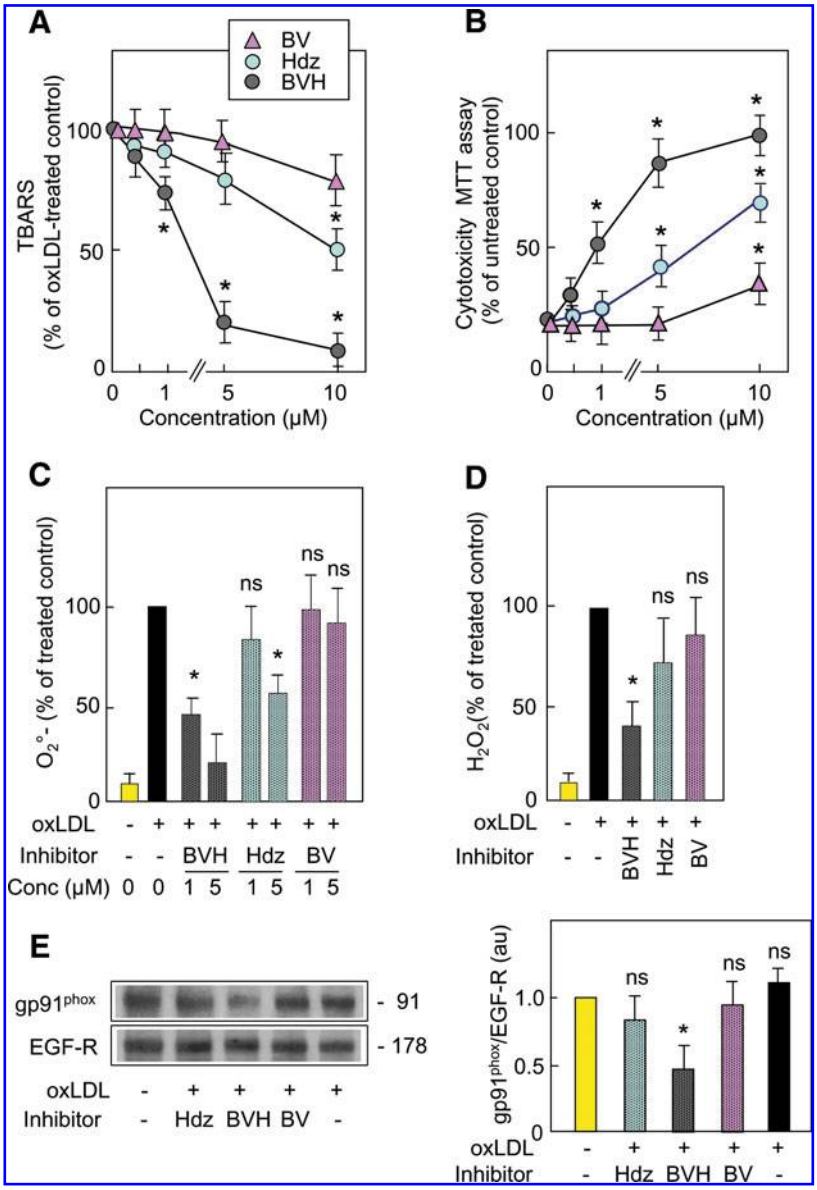

FIG. 3. BVH inhibits cell-induced LDL oxidation and the extracellular generation of reactive oxygen species (ROS). (A) Cell-mediated LDL oxidation was evaluated on human microvascular endothelial cell-1 (HMEC-1) seeded in 12-multiwell plates. The standard culture medium was removed and replaced by serum-free RPMI 1640 containing native LDL (100 μg apoB/ml) and the agents (BVH, Hdz, and BV) used at the indicated concentrations. After 14 h incubation at 37°C, the TBARS content was determined in the LDL-containing medium. Results are expressed as percent of the control incubated with LDLs in the absence of drug (the TBARS content of the oxidized LDL [oxLDL]-containing culture medium was 15 nmol/mg apoB ± 2.5). **(B)** Determination of HMEC-1 viability after 14 h of incubation in the presence of native LDLs and copper (1 μmol), as indicated in **(A)**. Cell viability was determined by the MTT test. Results are expressed as percent of the untreated control. **(C)** Determination of $O_2^{\cdot -}$ generation by HMEC-1 incubated for 1 h with oxLDL (100 μg/ml) ± the indicated agents (1 and 5 μM). $O_2^{\cdot -}$ was measured by the SOD-inhibitable reduction of cytochrome C, as reported in the Materials and Methods section. Results are expressed as percent of the control treated with oxLDLs. **(D)** Determination of H_2O_2 generation in the extracellular medium of HMEC-1 incubated for 30 min with oxLDL (100 μg/ml) ± the indicated agents (5 μM). H_2O_2 was evaluated by the HRP-dependent quenching of scopoletin fluorescence (ex/em 358/448 nm), measured as indicated in the Materials and Method section. Results are expressed as percent of the control treated with oxLDLs. **(E)** *Left panel*: Expression of the $gp91^{phox}$ subunit of NAD(P)H oxidase, evaluated by Western blot experiments from HMEC-1 incubated for 5 h with oxLDLs (100 μg/ml) ± the agents (BVH, Hdz, and BV), and revealed with a $gp91^{phox}$ anti antibody and anti EGF-receptor (EGF-R) (Santa-Cruz), as control. *Right panel*: densitometric analysis of $gp91^{phox}$ Western blot experiments by ImageJ software. $Gp91^{phox}$/EGF-R ratio was calculated and expressed in arbitray units (au), as mean ± SEM of four separate experiments. *$p < 0.05$ (values compared to the unstimulated control). In **(A–E)**, the data are mean ± SEM of four separate experiments. *$p < 0.05$. In **(C, D)**, compared to the oxLDL-treated control, black bar. The yellow bars represent the untreated control. (To see this illustration in color the reader is referred to the web version of this article at www.liebertonline.com/ars).

lipid peroxidation and subsequent toxicity (Fig. 3A, B). It may be noted that hydralazine was less efficient than BVH (Fig. 3A–D). BV did not exert any protective effect at the used concentrations.

The generation of extracellular ROS by NAD(P)H oxidase and its implication in LDL oxidation and atherosclerosis have been largely investigated (19, 20, 46). This functionally active NAD(P)H oxidase contains the membrane-bound subunits $p22^{phox}$ and $gp91^{phox}$ (20), and is required for the proliferation and migration of these cells (20, 60). The expression of $gp91^{phox}$ is increased and regulated by oxidative stress (20, 46), and is blocked by antioxidants such as resveratrol (8). Moreover, we previously reported that NAD(P)H oxidase is involved in the generation of extracellular ROS in HMEC-1 (11). We thus checked whether oxLDLs (preoxidized by UV irradiation/Cu in the absence of drug) increase the expression of $gp91^{phox}$ at the plasma membrane, and whether these responses are regulated by BVH and the other tested compounds. As shown in Figure 3E, oxLDLs increased the expression of $gp91^{phox}$ (the data in Fig. 3E were observed after 5 h incubation). All these responses were inhibited by BVH (and at a lesser extent by hydralazine) (both being tested at 5 μM), as well as by the metal chelator desferal, and by trolox (data not shown). BV had no inhibitory effect. Thus, it can be speculated that BVH inhibits the generation of extracellular ROS *via* a direct mechanism including its radical scavenger

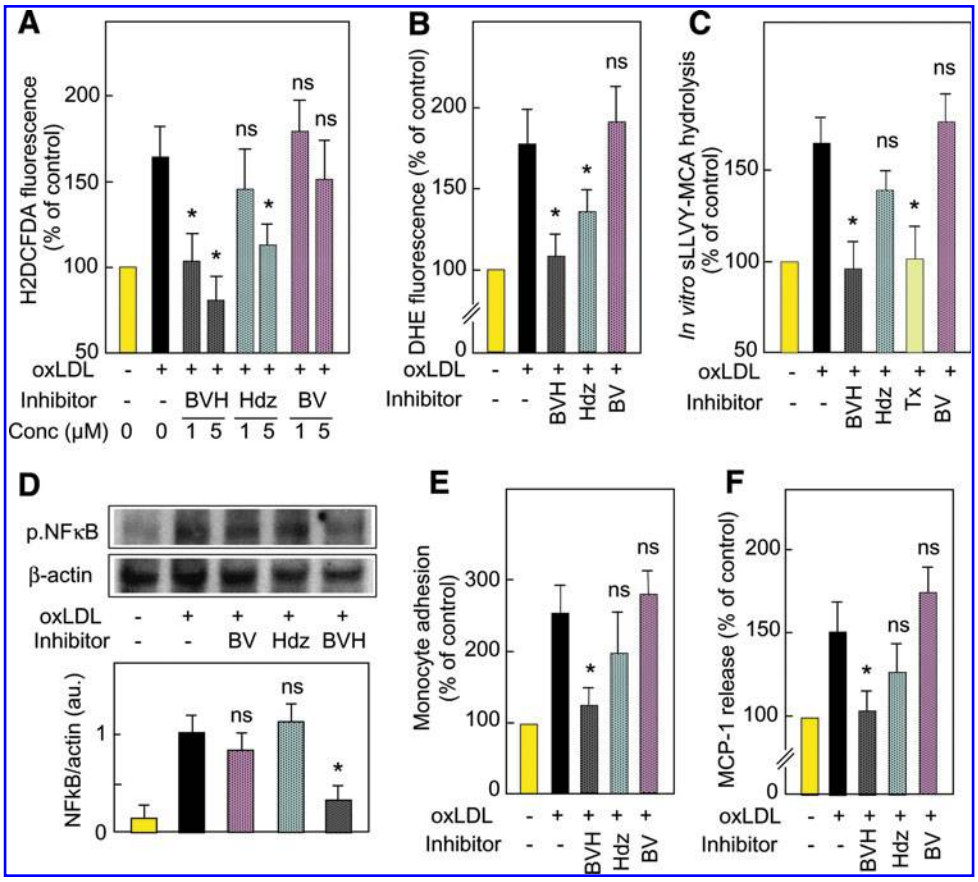

FIG. 4. BVH inhibits the intracellular oxidative stress and the release of MCP-1. (A, B) Rise of intracellular ROS triggered by oxLDLs (200 μg/ml, 3 h incubation) and inhibition by BVH, Hdz, and BV. HMEC-1 were incubated with or without oxLDLs (200 μg/ml for 3 h) and the indicated agent, used at 1 or 5 μM **(A)** or at 5 μM **(B)**. Thirty minutes before the end of the experiment, cells were loaded with the ROS-sensitive fluorescent probes 6-carboxy-2′,7′-dichlorodihydrofluorescein diacetate, di(acetoxymethyl ester) (H_2DCFDA-AM) **(A)** or dihydroethidium (DHE) **(B)** and the fluorescence of the cells was measured as indicated in the Materials and Methods section. **(C)** Activation of the 20S proteasome determined by measuring the hydrolysis of the sLLVY-MCA substrate, by lysates from cells incubated for 2 h with 200 μg/ml of oxLDL (as described in the Materials and Methods section), and effect of BVH, Hdz, BV, and trolox (Tx) as control (all were tested at 5 μM, except trolox, 10 μM). **(D)** *Upper panel*: Western blot experiments showing the phosphorylation of NF-κB, upon 2 h stimulation of HMEC-1 with toxic oxLDL concentrations (200 μg/ml), and effect of BVH, Hdz and BV (all the agents were tested at 5 μM). *Lower panel*: densitometric analysis of phospho-NF-κB Western blot experiments by ImageJ software. Phospho-NF-κB/β-actin ratio was calculated and expressed in arbitray units (au), as mean $\pm$ SEM of four separate experiments. *$p < 0.05$ (values compared to the unstimulated control). **(E)** Monocytes adhesion to HMEC-1 activated by oxLDLs. HMEC-1 were grown on 12-multiwell culture plaques, and stimulated by oxLDLs for 1–4 h. The adhesion assay was performed using Raw-267.4 macrophages previously loaded with calcein (5 μM) for 10 min and washed three times in warm PBS. The fluorescent calcein-loaded macrophages (50,000 cellules/well) were added to HMEC-1 culture for 30 min, and then the cells were carefully washed with warm PBS and lyzed in water, and the fluorescence of the mixture was immediately measured (ex/em 490/525). The results are expressed as percentage of the unstimulated control. **(F)** MCP-1 release by HMEC-1 activated by oxLDLs. HMEC-1 were incubated with oxLDLs (200 μg/ml) for 1 to 5 h, and MCP-1 released in the culture medium was determined by ELISA. The data are expressed as percentage of the unstimulated control. In **(A–F)**, the data are means $\pm$ SEM of four separate experiments. *$p < 0.05$; compared to the oxLDL-treated control, black bar. The yellow bars represent the untreated control. (To see this illustration in color the reader is referred to the web version of this article at www.liebertonline.com/ars).

and metal chelator properties, and indirectly, by blocking the increase in gp91phox expression.

We then investigated whether BVH is able to inhibit the intracellular ROS rise generated by oxLDLs, and involved in vascular dysfunction, inflammatory response, and cytotoxicity (1, 44, 45). For this purpose, HMEC-1 were loaded with two permeant ROS-sensitive probes, the H_2DCFDA-AM probe that reacts with hydroperoxides, and DHE that is more specific for $O_2^{\cdot -}$ (18). Incubation of HMEC-1 with toxic concentration of oxLDLs (200 μg/ml) resulted in increased level in cellular hydroperoxides and $O_2^{\cdot -}$, which were completely prevented by BVH (1–5 μM) (Fig. 4A, B), whereas no or only very weak protective effects were obtained with similar concentrations of hydralazine and BV.

Oxidative stress and oxLDLs trigger a proinflammatory signaling, which results (at least in part) from the activation of the redox-sensitive NF-κB transcription factor (44). The nuclear translocation of NF-κB depends on its phosphorylation, and on the proteasomal degradation of IκBα, the cytosolic constitutive inhibitor of NF-κB (44). The incubation of HMEC-1 with oxLDLs stimulated the *in vitro* hydrolysis of sLLVY-MCA (a fluorogenic synthetic peptide substrate for 20S proteasome) (Fig. 4C) and the phosphorylation of NF-κB (Fig. 4D) (the reported data were observed at 2 h), in agreement with our previous report (61). These responses were completely inhibited by BVH, whereas hydralazine and BV had no effect. The proinflammatory signaling resulting from NF-κB activation is implicated in the expression of adhesion molecules and the secretion of chemoattractants (9, 51, 56). To check whether BVH inhibits the proinflammatory signaling of oxLDLs, we tested its ability to inhibit the monocyte recruitment to the endothelium activated by oxLDLs. As shown in Figure 4E, a significant increase in monocyte adhesion to the endothelium was observed after incubation of cells with

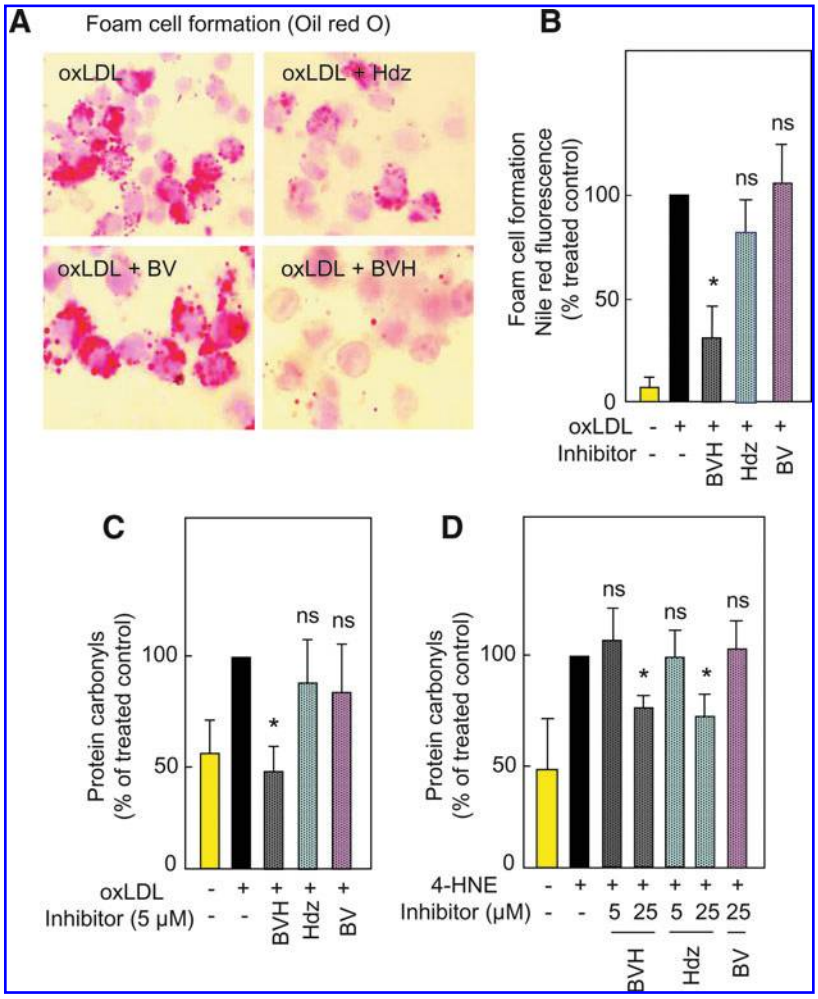

FIG. 5. BVH inhibits foam cell formation and the carbonyl stress. **(A, B)** Inhibition of foam cell formation by BVH. Raw264.7 murine macrophages were incubated for 14 h with oxLDLs (100 μg/ml) and the tested agents BVH, Hdz, or BV (each used at the final concentration of 5 μM). In **(A)**, the cells were washed twice, fixed in 4% paraformaldehyde, and stained with oil Red O, and observed microscopically. Representative of three separate experiments. In **(B)** Raw264.7 were stained with Nile Red, scrapped, and the fluorescence of the cells was measured as indicated in the Materials and Methods section. Results are expressed as percentage of the control treated by oxLDLs (without added drug, black bars). **(C)** Protein carbonyl content increase induced by oxLDLs, and inhibition by BVH. The protein carbonyl content was determined on cell extracts after 14 h incubation of HMEC-1 with oxLDLs (200 μg/ml) used either alone or in the presence of BVH, Hdz, and BV (5 μM final concentration). Carbonylated proteins were determined spectrophotometrically using DNPH as described in the Materials and Methods section. The results are expressed as percent of the control treated by oxLDLs (without drug, black bars). **(D)** Protein carbonyl content increase induced by 4-hydroxynonenal (4-HNE) (10 μM, 14 h) and inhibitory effect of BVH and Hdz. These data are means ± SEM of four separate experiments (*$p < 0.05$; compared to the oxLDL-treated control, black bar). The yellow bars represent the untreated control. (To see this illustration in color the reader is referred to the web version of this article at www.liebertonline.com/ars).

oxLDLs. This effect was prevented by BVH, but not by hydralazine nor BV. Likewise, the secretion of MCP-1 was inhibited by BVH, but not or only weakly by hydralazine or BV (Fig. 4F). Altogether, these data indicate that BVH exerts a potent antioxidant activity able to prevent the rise of extra- and intracellular ROS. Moreover, BVH inhibits the inflammatory signaling mediated by oxLDLs, as assessed by the inhibition of NF-κB, and the reduced expression of $gp91^{phox}$, adhesion molecules, and chemoattractant factors.

BVH inhibit foam cell and carbonyl stress induced by oxLDLs

The formation of foam cells results from the uptake by macrophages of modified and oxLDLs (55). Foam cell formation was evaluated in murine Raw 264.7 macrophages incubated for 14 h with 100 μg/ml oxLDLs and the tested agents (5 μM). The lipid accumulation was evidenced by oil red O staining and was fluorometrically quantified by Nile Red. Foam cell formation was strongly inhibited by BVH, but not by BV, whereas hydralazine exhibited only weak protection (Fig. 5A, B) (higher concentrations being required for preventing foam cell formation) (16).

We then investigated whether BVH may block the modification by carbonylation of cellular proteins (53), which can be protected by carbonyl scavengers (16). As shown in Figure 5C, BVH prevented the cellular increase in protein carbonyl content induced by oxLDLs (200 μg/ml, 14 h incubation), whereas hydralazine and BV were unefficient at the used concentration (5 μM). As shown in Figure 5D, 4-HNE (10 μM) directly added to the culture medium of HMEC-1 triggered an increase in protein carbonyl content, which was blocked by BVH and hydralazine, but not by BV. The protection against the carbonyl stress induced by 4-HNE necessited higher BVH and hydralazine concentrations (25 μM), whereas the antioxidant properties of BVH were observed from 1 to 5 μM. Taken together, it is suggested that the inhibitory effect of BVH on the carbonyl stress elicited by oxLDLs mainly results from its antioxidant properties, whereas its intrinsic carbonyl scavenger properties are comparable with those exerted by hydralazine.

BVH prevents oxLDL-mediated apoptosis

The antiapoptotic properties of BVH, hydralazine, and BV were evaluated on HMEC-1 incubated with toxic concentrations of oxLDLs. After 24 h incubation, the residual viability of cells (evaluated by the MTT test) was < 20% of the control (cells incubated without oxLDLs) (Fig. 6A). Dose–response experiments indicated that BVH was strongly efficient even at low concentrations (1 μM) for preventing the toxic effect of oxLDLs, whereas 5 μM

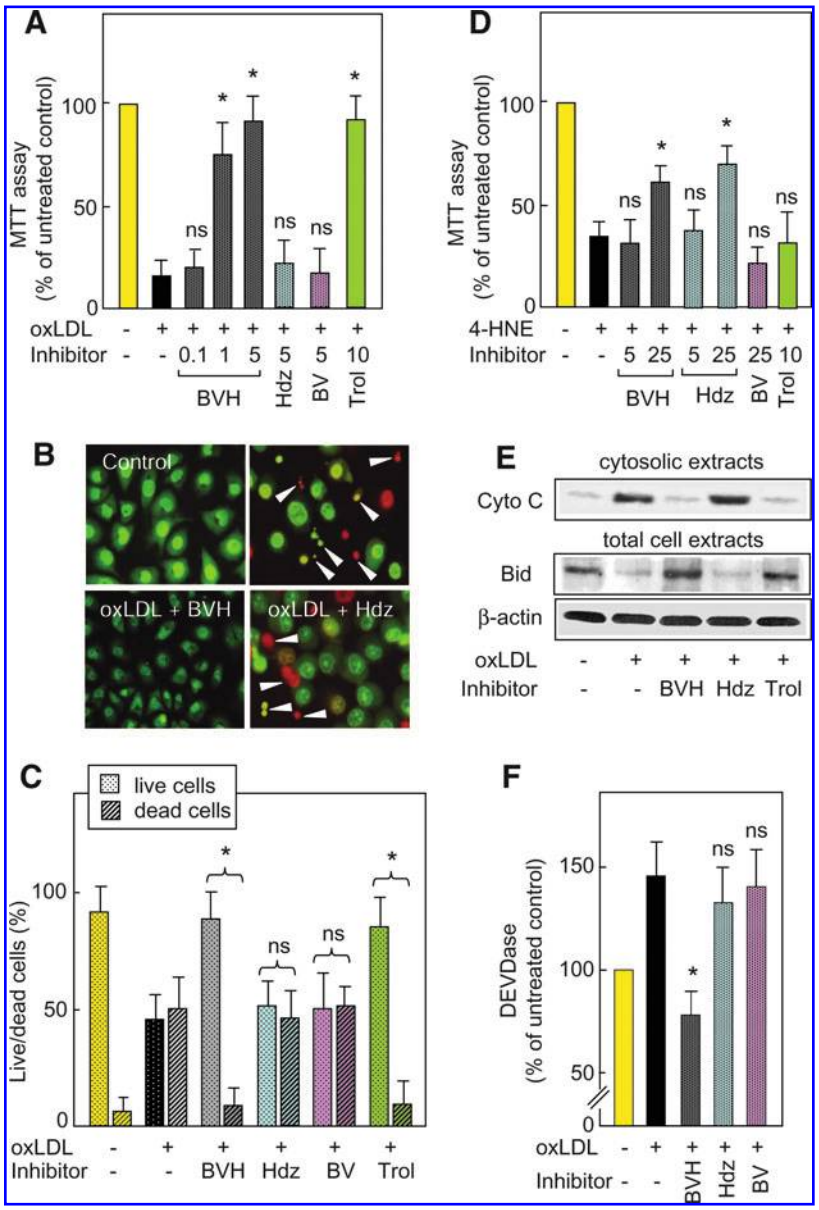

FIG. 6. BVH prevents oxLDL-mediated apoptotic signaling. (A–C) Cytoprotective effect of BVH. Sub-confluent HMEC-1 were incubated in serum-free culture medium with oxLDLs (200 μg apoB/ml) and the tested agents. **(A)** Cytotoxicity and cytoprotection were evaluated by the MTT assay, after 24 h incubation with oxLDLs and with/without the tested agents (used at the indicated concentrations). The results are expressed as percentage of the untreated control. Fluorescence microscopy **(B)** and count of live and dead cells **(C)** incubated for 16 h with/without oxLDLs (200 μg/ml) and with/without BVH (5 μM), Hdz (5 μM), BV (5 μM), and trolox (Trol, 10 μM). Cells were stained by the fluorescent DNA intercalating agents Syto-13 (permeant, green) and propidium iodide (nonpermeant, red), and examined by fluorescence microscopy that reveals live cells (green with normal nucleus) and dead cells with apoptotic nucleus (green apoptotic or red postapoptotic necrosis, *arrows*) or primary necrosis with red nucleus (without apoptotic features). In **(B)**, representative of three separate experiments. **(D)** Cytoprotective effect of BVH, Hdz, and BV (5 and 25 μM) on the toxicity of 4-HNE (10 μM, 14 h incubation), and evaluated by the MTT test as percentage of the untreated control. **(E, F)** BVH blocks the proapoptotic cascade elicited by oxLDLs in HMEC-1 (similar experimental conditions as in **(C). (E)** Western blots of cytochrome C (cyto C) on cytosolic proteins, and Bid and β-actin on total cell extracts. Representative of four separate experiments. **(F)**. Evaluation of the DEVDase activity on cell extracts using the fluorogenic substrate Ac-DEVD-AMC, as indicated in Materials and Methods section. The results are expressed as percentage of the untreated controls. These data are means $\pm$ SEM of at least four separate experiments. *$p < 0.05$ (comparison to the oxLDL-treated controls, black bars). The yellow bars represent the untreated control. (To see this illustration in color the reader is referred to the web version of this article at www.liebertonline.com/ars).

hydralazine and BV had no protective effect (Fig. 6A). Cell death was characterized by counting apoptotic cells after double staining with two fluorescent intercalating agents, the permeant DNA probe syto-13 that stains green all the nuclei, and propidium iodide (PI) that stains red only cells with permeabilized membrane (*i.e.*, necrotic cells affected by either primary necrosis or postapoptotic necrosis) (47, 62). As shown in Figure 6B and C, oxLDLs increased the number of apoptotic cells. BVH (1–5 μM) prevented the apoptosis of HMEC-1 cells, whereas hydralazine and BV (1–5 μM) were unefficient. BVH (5 μM) blocked the apoptotic signaling elicited by oxLDLs (Fig. 6E, F), by inhibiting the cleavage of Bid and the cytosolic release of cytochrome C, as well as the activation of DEVDase (caspase 3). BVH and hydralazine (25 μM), but not BV, blocked the carbonyl stress-induced toxicity, by inhibiting cell death elicited by pure 4-HNE (10 μM) added to the culture medium of HMEC-1 (Fig. 6D). The protective effect of BVH on 4-HNE-induced cell death necessited higher concentrations (25 μM), and was comparable with that exerted by hydralazine (Fig. 6D). Trolox, an antioxidant deriving from vitamin E, and used as control, blocked oxLDL-mediated apoptosis in agreement with previous studies (33), but had no effect on 4-HNE-induced cytotoxicity.

BVH prevents the development of atherosclerosis in apoE$^{-/-}$ mice

The deletion of the *apoE* gene in apoE$^{-/-}$ mice leads to severe hypercholesterolemia and spontaneous atherosclerosis, even on a standard chow diet (65). Three groups of 20 apoE$^{-/-}$ mice (male) received a standard diet chow, and were either untreated (control) or treated for 16 weeks with BVH or hydralazine added to the drinking water. Blood pressure,

Table 1. Plasma Cholesterol, Triglyceride, and Glycemia Concentrations and Blood Pressure in apoE$^{-/-}$ Mice After 16 Weeks of Treatment with Bisvanillyl-Hydralazone and Hydralazine

ApoE$^{-/-}$ mice treatment	*Glucose (mM)*	*Total cholesterol (mM)*	*TG (mM)*	*BP (mmHg)*
Untreated	8.6 ± 0.4^a	13.8 ± 1.6^a	1.58 ± 0.4^a	108 ± 5
BVH	8.2 ± 0.3^a	13.4 ± 1.4^a	1.76 ± 0.3^a	110 ± 6
Hydralazine	8.5 ± 0.3^a	13.7 ± 1.5^a	1.45 ± 0.3^a	107 ± 4

Results are given as mean ± SD.
[a]$p < 0.05$ for comparison between untreated and drug-treated apoE$^{-/-}$ mice, 20 animals per group.
BVH, bisvanillyl-hydralazone; BP, blood pressure; TG, triglycerides.

plasmatic levels of total cholesterol, triglycerides, and glucose were comparable in treated and untreated animals (Table 1), thereby indicating that neither BVH nor hydralazine modify the blood level of circulating lipids. In untreated (control) apoE$^{-/-}$ mice, the area of atherosclerotic lesions in aortic sinus was $24{,}550 \pm 6340\ \mu m^2$, in agreement with (16). BVH administration resulted in a marked reduction (>55%) of the atherosclerotic lesion area (Fig. 7A). By comparison, hydralazine reduced by 40% the size of the lesions, as previously reported (16). In the light of the antioxidant and anti-inflammatory properties of BVH, we checked the composition of atherosclerotic lesions from BVH-treated and control animals. As shown in Figure 7B, BVH reduced the tissular expression of the chemoattractant factor MCP-1, and the number of α-actin-positive cells (SMC), as well as CD68-positive cells (macrophages) (data not shown). BVH also reduced lymphocyte infiltration (as assessed by a decrease in CD3-positive T cells), and inhibited the accumulation of 4-HNE adducts on tissular proteins (carbonyl stress) in aortic sinus of apoE$^{-/-}$ mice (Fig. 7B). These data were confirmed by the reduction by BVH (and hydralazine) of the tissular increase in protein carbonyl content (Fig. 7C), and by the decrease in 4-HNE-adduct accumulation on the PDGF receptor (a target of carbonyl stress) (13, 62), in aortas of treated *versus* untreated animals (Fig. 7D).

Discussion

Oxidative stress, LDL oxidation, and carbonyl stress are involved in the initiation of early atherosclerotic lesions, and

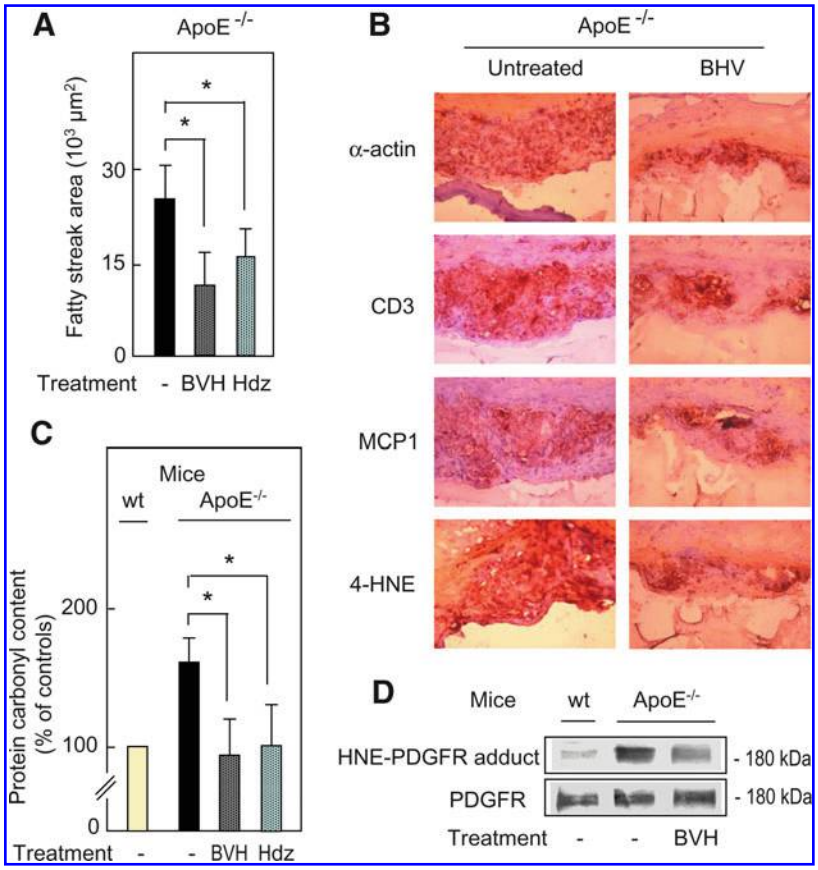

FIG. 7. Antiatherogenic effect of BVH on ApoE$^{-/-}$ mice lesions. ApoE$^{-/-}$ male mice aged 4 weeks (20 in each group) were fed a regular mouse chow diet and treated or not by BVH or Hdz (30 mg/l, *i.e.*, 10 mg/kg/day added to the drinking water) for 16 weeks. Hearts were embedded in OCT (Tissue-Tek) and aortic sinus were cut into 10 µm sections, stained with oil Red O, and counterstained with hematoxylin–eosin, and a morphometric quantification of the lesion size was performed, as indicated in the Materials and Methods section. **(A)** Fatty streak area quantification. Means ± SEM of fatty streak area in aortic sinus of untreated male mice was $24{,}550 \pm 6340\ \mu m^2$. **(B)** Immunohistochemistry of cryosections of aortic sinus from untreated (left) and BVH-treated (right) apoE$^{-/-}$ mice. From top to bottom, α-actin (SMC), CD3 (T lymphocytes), MCP-1, and 4-HNE-adduct (HNE) immunostaining. The pictures showed here are representative of five separate untreated and BVH-treated mice. **(C)** Determination of the protein carbonyl content in protein extracts from aortas of control untreated, BVH-, and Hdz-treated mice. **(D)** Western blot experiments of HNE-adduct accumulation in aortas of control and BVH-treated mice. These results are representative of three separate experiments. In **(A, C)**, the data are means ± SEM of 20 mice in each group. *$p < 0.05$ (comparison to the untreated controls, black bars). The yellow bars represent the untreated control. (To see this illustration in color the reader is referred to the web version of this article at www.liebertonline.com/ars).

in the inflammatory and apoptotic events involved in the progression of atherosclerosis (3, 4, 23, 25). Antioxidants prevent the development of fatty streaks in animals (3, 24, 37), but their efficacy on advanced atherosclerotic lesions and on cardiovascular events in humans is debated (3, 5, 63). Although the efficiency of carbonyl scavengers on LDL oxidation (27) and on the late steps of atherosclerosis is not clarified, inhibiting both oxidative stress and carbonyl stress may represent a new therapeutic strategy for atherosclerosis. Carbonyl scavengers are usually poor antioxidants, whereas antioxidants fail to neutralize carbonyl compounds once adducts are formed on proteins (40, 42). We recently reported that hydrazine derivatives used in medicine inhibit the carbonyl stress induced by oxLDL, and slow down the development of atherosclerotic lesions in apoE$^{-/-}$ mice (this being correlated with a decrease in foam cell formation). Among these agents, the antihypertensive drug hydralazine is a carbonyl scavenger agent with (moderate) antioxidant activity (16). To improve the antioxidant properties of hydralazine, we designed and synthesized BVH, a hydralazine derivative, exhibiting both antioxidant (presence of a phenolic moiety) and carbonyl scavenger properties (presence of hydralazine). The linker between BV and hydralazine is an acid-labile hydrazone group that was designed to undergo hydrolysis, allowing the release of hydralazine under physiological conditions (28).

A first observation is that BVH is a potent antioxidant, associating both metal chelator and radical scavenger properties. BVH (even at low concentrations) formed complexes with copper, and significantly blocked the copper-induced and AAPH-induced LDL oxidation, (which is metal-independent), as well as LDL oxidation mediated by vascular cells (HMEC-1), which depends on the presence of transition metal. The later mimicks the mechanism of LDL oxidation occurring *in vivo* in the vascular wall, since copper ions are present in the vessels, and contribute in the generation of oxLDLs and atherogenesis (3, 25, 64). The metal chelator and radical scavenger properties of BVH allow to block the generation of extracellular ROS that are involved in cell-mediated LDL oxidation ($O_2^{\circ -}$ initiates the generation of H_2O_2 and OH°, formed through the Fenton reaction in the presence of iron or copper) (29). The copper-chelating properties of BVH should help to inhibit the Fenton reaction as assessed by the inhibition of H_2O_2 secretion in the culture medium. These effects are reinforced by the inhibitory effect of BVH on the expression of the gp91^{phox} subunit of NADPH-oxidase, in agreement with reports showing the role of gp91^{phox} in extracellular ROS generation (19, 20). The inhibitory effect of BVH on gp91^{phox} expression could result from an inhibition by BVH, of the redox sensitive proinflammatory NF-κB transcription factor, which regulates the expression of NAD(P)H oxidase (2, 17), and is activated by oxLDLs (1). These data are in agreement with the classical inhibitory effect of antioxidants on the intracellular oxidative stress, the proteasome activation (as reported here with BVH), and the proteasomal degradation of I-κB, the natural cytosolic inhibitor of NF-κB (44). Besides, BVH inhibited the proinflammatory signaling mediated by oxLDLs (44, 47), leading to stress-mediated cellular responses, such as the adhesion of monocytes to HMEC-1 stimulated by oxLDL, and the secretion of the chemoattractant MCP-1 involved in mononuclear cell recruitment (9, 44). Interestingly, BVH prevented oxLDL cytotoxicity, by blocking the apoptotic signaling resulting in the activation of the intrinsic mitochondrial apoptotic cascade (characterized by the cleavage of the proapoptotic factor Bid, the release of cytochrome C, and the activation of caspase 3) (47). These data are in agreement with the generally known cytoprotective properties of antioxidants (vitamin E, Trolox, probucol, phenolic acids, and flavonoids) (34, 37, 57). The antioxidant effect of BVH was not reproduced by co-incubating BV and hydralazine, thereby suggesting that the effect of BVH results from a conformational change in the chemical structure of its components, which confers to the molecule a better access to its targets (ROS, copper), and its subsequent antioxidant and cytoprotective properties.

The second observation is that BVH exhibited carbonyl scavenger properties similar to those observed for hydralazine, and evidenced by the inhibitory effect of BVH on protein carbonylation and toxicity elicited by 4-HNE directly added to the culture medium of HMEC-1 (which triggers a carbonyl stress independent of lipid peroxidation). Trolox used as control cytoprotective antioxidant was unable to block the carbonyl stress induced by 4-HNE, and this suggests that the carbonyl scavenger properties of BVH (on the direct formation of 4-HNE-adducts) are independent of its antioxidant activity. These effects of BVH necessite relatively higher concentrations (25 μM), and are comparable with (thus probably result from) hydralazine, which is an hydrazine derivative, and a strong carbonyl scavenger (45). One hypothesis is that BVH undergoes hydrolysis of its acid-labile hydrazone group, thereby releasing hydralazine at acidic pH under physiological conditions (28). In contrast, the strong inhibitory effect of low BVH concentrations (1–5 μM) on the formation of protein carbonyls and foam cell accumulation induced by oxLDLs likely resulted from its antioxidant and cytoprotective rather than carbonyl scavenger properties. Nevertheless, it can be speculated that BVH is protective through its antioxidant properties (inhibition of oxidative stress, inflammation, and apoptosis induced by oxLDLs), and through its carbonyl scavenger properties at least in the vascular wall of apoE$^{-/-}$ mice, where it prevented the accumulation of HNE-adducts on PDGF-R, a known target of carbonyl stress (13, 62). The antiatherogenic effect of BVH in apoE$^{-/-}$ mice was superior to that of hydralazine (55%–60% of lesion area decrease *vs.* 40%–45% for hydralazine), perhaps because of its better antioxidant properties. BVH did not reduce the plasma lipid content of apoE$^{-/-}$ mice, but prevented in part the accumulation of macrophagic foam cells, CD3 T-cell infiltration, and MCP-1 expression. The protein carbonyl content and the accumulation of 4-HNE adducts on tissular proteins (such as PDGFR) were reduced in BVH-treated apoE$^{-/-}$ mice, indicating a good correlation of these parameters with the decrease in fatty streaks accumulation and plaque size reduction.

In conclusion, BVH is a potent antiatherogenic agent, and represents the prototype of new antioxidant and carbonyl scavenger molecules, which should be of interest for slowing down the progression of early atherosclerotic lesions formation, and more generally of pathologies associated with oxidative and carbonyl stress.

Financial Support and Acknowledgments

The authors acknowledge the financial support by INSERM, CNRS, Université Paul Sabatier, Fondation Coeur et Artères (FCA-06T6), Fondation pour la Recherche Médicale (DCV2007040927), and European COST-B35. Dr. Gallet (SNCF Laboratory, Toulouse) is gratefully acknowledged for providing human sera. The authors thank Mrs. Corinne Bernis for her excellent technical assistance.

Benaissa Bouguerne is recipient of support from the Ministère de l'Enseignement Supérieur et de la Recherche. Nadji Belkheiri is recipient of a grant from Algerian government.

Author Disclosure Statement

No competing financial interests exist.

References

1. Andalibi A, Liao F, Imes S, Fogelman AM, and Lusis AJ. Oxidized lipoproteins influence gene expression by causing oxidative stress and activating the transcription factor NF-kappa B. *Biochem Soc Trans* 21(Pt 3): 651–655, 1993.
2. Anrather J, Racchumi G, and Iadecola C. NF-kappaB regulates phagocytic NADPH oxidase by inducing the expression of gp91phox. *J Biol Chem* 281: 5657–5667, 2006.
3. Aviram M. Review of human studies on oxidative damage and antioxidant protection related to cardiovascular diseases. *Free Radic Res* 33, Suppl: S85–S97, 2001.
4. Berliner JA and Heinecke JW. The role of oxidized lipoproteins in atherogenesis. *Free Radic Biol Med* 20: 707–727, 1996.
5. Brigelius-Flohe R, Kluth D, and Banning A. Is there a future for antioxidants in atherogenesis? *Mol Nutr Food Res* 49: 1083–1089, 2005.
6. Bucciarelli LG, Wendt T, Qu W, Lu Y, Lalla E, Rong LL, Goova MT, Moser B, Kislinger T, Lee DC, Kashyap Y, Stern DM, and Schmidt AM. RAGE blockade stabilizes established atherosclerosis in diabetic apolipoprotein E-null mice. *Circulation* 106: 2827–2835, 2002.
7. Chait A and Heinecke JW. Lipoprotein modification: cellular mechanisms. *Curr Opin Lipidol* 5: 365–370, 1994.
8. Chow SE, Hshu YC, Wang JS, and Chen JK. Resveratrol attenuates oxLDL-stimulated NADPH oxidase activity and protects endothelial cells from oxidative functional damages. *J Appl Physiol* 102: 1520–1527, 2007.
9. Cominacini L, Garbin U, Pasini AF, Davoli A, Campagnola M, Contessi GB, Pastorino AM, and Lo Cascio V. Antioxidants inhibit the expression of intercellular cell adhesion molecule-1 and vascular cell adhesion molecule-1 induced by oxidized LDL on human umbilical vein endothelial cells. *Free Radic Biol Med* 22: 117–127, 1997.
10. Cossarizza A, Ferraresi R, Troiano L, Roat E, Gibellini L, Bertoncelli L, Nasi M, and Pinti M. Simultaneous analysis of reactive oxygen species and reduced glutathione content in living cells by polychromatic flow cytometry. *Nat Protoc* 4: 1790–1797, 2009.
11. de Souza JA, Vindis C, Nègre-Salvayre A, Rye KA, Couturier M, Therond P, Chantepie S, Salvayre R, Chapman MJ, and Kontush A. Small, dense HDL 3 particles attenuate apoptosis in endothelial cells: pivotal role of apolipoprotein A-I. *J Cell Mol Med* 14: 608–620, 2010.
12. Duval C, Cantero AV, Auge N, Mabile L, Thiers JC, Negre-Salvayre A, and Salvayre R. Proliferation and wound healing of vascular cells trigger the generation of extracellular reactive oxygen species and LDL oxidation. *Free Radic Biol Med* 35: 1589–1598, 2003.
13. Escargueil-Blanc I, Salvayre R, Vacaresse N, Jürgens G, Darblade B, Arnal JF, Parthasarathy S, and Nègre-Salvayre A. Mildly oxidized LDL induces activation of platelet-derived growth factor beta-receptor pathway. *Circulation* 104: 1814–1821, 2001.
14. Esterbauer H, Schaur RJ, and Zollner H. Chemistry and biochemistry of 4-hydroxy nonenal, malonaldehyde and related aldehydes. *Free Radic Biol Med* 11: 81–128, 1991.
15. Fang YZ, Yang S, and Wu G. Free radicals, antioxidants, and nutrition. *Nutrition* 18: 872–879, 2002.
16. Galvani S, Coatrieux C, Elbaz M, Grazide MH, Thiers JC, Parini A, Uchida K, Kamar N, Rostaing L, Baltas M, Salvayre R, and Nègre-Salvayre A. Carbonyl scavenger and antiatherogenic effects of hydrazine derivatives. *Free Radic Biol Med* 45: 1457–1467, 2008.
17. Gauss KA, Nelson-Overton LK, Siemsen DW, Gao Y, DeLeo FR, and Quinn MT. Role of NF-kappaB in transcriptional regulation of the phagocyte NADPH oxidase by tumor necrosis factor-alpha. *J Leukoc Biol* 82: 729–741, 2007.
18. Georgiou CD, Papapostolo I, Patsoukis N, Tsegenidis T, and Sideris T. An ultrasensitive fluorescent assay for the *in vivo* quantification of superoxide radical in organisms. *Anal Biochem* 347: 144–151, 2005.
19. Görlach A, Brandes RP, Nguyen K, Amidi M, Dehghani F, and Busse R. A gp91phox containing NADPH oxidase selectively expressed in endothelial cells is a major source of oxygen radical generation in the arterial wall. *Circ Res* 87: 26–32, 2000.
20. Griendling KK, Sorescu D, and Ushio-Fukai M. NAD(P)H oxidase: role in cardiovascular biology and disease. *Circ Res* 86: 494–501, 2000.
21. Grune T, Reinheckel T, and Davies KJA. Degradation of oxidized proteins in K562 human hematopoietic cells by proteasome. *J Biol Chem* 271: 15504–15509, 1996.
22. Harkewicz R, Hartvigsen K, Almazan F, Dennis EA, Witztum JL, and Miller YI. Cholesteryl ester hydroperoxides are biologically active components of minimally oxidized low density lipoprotein. *J Biol Chem* 283: 10241–10251, 2008.
23. Heinecke JW. Oxidants and antioxidants in the pathogenesis of atherosclerosis: implications for the oxidized LDL hypothesis. *Atherosclerosis* 141: 1–15, 1998.
24. Hishikawa K, Nakaki T, and Fujita T. Oral flavonoid supplementation attenuates atherosclerosis development in apolipoprotein E-deficient mice. *Arterioscler Thromb Vasc Biol* 25: 442–446, 2005.
25. Holvoet P and Collen D. Oxidized lipoproteins in atherosclerosis and thrombosis. *FASEB J* 8: 1279–1284, 1994.
26. Ichihashi K, Osawa T, Toyokuni S, and Uchida K. Endogenous formation of protein adducts with carcinogenic aldehydes: implications for oxidative stress. *J Biol Chem* 276: 23903–23913, 2001.
27. Jedidi I, Therond P, Zarev S, Gardès-Albert M, Legrand A, Barouki R, Bonnefont-Rousselot D, and Aggerbeck M. Paradoxical protective effect of aminoguanidine toward LDL oxidation: inhibition of apolipoprotein B fragmentation without preventing its carbonylation. Mechanism of action of aminoguanidine. *Biochemistry* 42: 11356–11365, 2003.
28. Kalia J and Raines RT. Hydrolytic stability of hydrazones and oximes. *Angew Chem* 120: 7633–7636, 2008.

29. Kritharides L, Jessup W, and Dean RT. Macrophages require both iron and copper to oxidize LDL in Hanks' balanced salt solution. *Arch Biochem Biophys* 323: 127–136, 1995.
30. Leonarduzzi G, Arkan MC, Basaga H, Chiarpotto E, Sevanian A, and Poli G. Lipid oxidation products in cell signaling. *Free Radic Biol Med* 28: 1370–1378, 2000.
31. Libby P, Ridker PM, and Maseri A. Inflammation and atherosclerosis. *Circulation* 105: 1135–1143, 2002.
32. Loschen G, Azzi A, and Flobe A. Mitochondrial H_2O_2 formation: relationship with energy conservation. *FEBS Lett* 33: 84–87, 1973.
33. Lusis AJ. Atherosclerosis. *Nature* 407: 233–241, 2000.
34. Mabile L, Fitoussi G, Periquet B, Schmitt A, Salvayre R, and Nègre-Salvayre A. Alpha-tocopherol and trolox block the early intracellular events (TBARS and calcium rises) elicited by oxidized low density lipoproteins in cultured endothelial cells. *Free Radic Biol Med* 19: 177–187, 1995.
35. McCord JM and Fridovich I. Superoxide dismutase. An enzymic function for erythrocuprein (hemocuprein). *J Biol Chem* 244: 6049–6055, 1969.
36. Mira L, Fernandez MT, Santos M, Rocha R, Florêncio MH, and Jennings KR. Interactions of flavonoids with iron and copper ions: a mechanism for their antioxidant activity. *Free Radic Res* 36: 1199–1208, 2002.
37. Moghadasian MH, McManus BM, Godin DV, Rodrigues B, and Frolich JJ. Proatherogenic and antiatherogenic effects of probucol and phytosterols in apolipoprotein E-deficient mice. *Circulation* 99: 1733–1739, 1999.
38. Munzel T, Kurz S, Rajagopalan S, Thoenes M, Berrington WR, Thompson JA, Freeman BA, and Harrison DG. Hydralazine prevents nitroglycerin tolerance by inhibiting activation of a membrane-bound NADH oxidase. A new action for an old drug. *J Clin Invest* 98: 1465–1470, 1996.
39. Napoli C. Oxidation of LDL, atherogenesis, and apoptosis. *Ann N Y Acad Sci* 1010: 698–709, 2003.
40. Negre-Salvayre A, Coatrieux C, Ingueneau C, and Salvayre R. Advanced lipid peroxidation end products in oxidative damage to proteins. Potential role in diseases and therapeutic prospects for the inhibitors. *Br J Pharmacol* 153: 6–20, 2008.
41. Perrin DD and Armarego WLF. *Purification of Laboratory Chemicals*, third edition. Oxford: Pergamon Press, 1988.
42. Peyroux J and Sternberg M. Advanced glycation endproducts (AGEs): pharmacological inhibition in diabetes. *Pathol Biol* (Paris) 54: 405–419, 2000.
43. Rader DJ and Puré E. Lipoproteins, macrophage function, and atherosclerosis: beyond the foam cell? *Cell Metab* 1: 223–230, 2005.
44. Robbesyn F, Salvayre R, and Negre-Salvayre A. Dual role of oxidized LDL on the NF-kappaB signaling pathway. *Free Radic Res* 38: 541–551, 2004.
45. Rollas S and Küçükgüzel SG. Biological activities of hydrazone derivatives. *Molecules* 12: 1910–1939, 2007.
46. Rueckschloss U, Duerrschmidt N, and Morawietz H. NADPH oxidase in endothelial cells: impact on atherosclerosis. *Antioxid Redox Signal* 5: 171–180, 2003.
47. Salvayre R, Auge N, Benoist H, and Negre-Salvayre A. Oxidized low-density lipoprotein-induced apoptosis. *Biochim Biophys Acta* 1585: 213–221, 2002.
48. Sanson M, Augé N, Vindis C, Muller C, Bando Y, Thiers JC, Marachet MA, Zarkovic K, Sawa Y, Salvayre R, and Nègre-Salvayre A. Oxidized low-density lipoproteins trigger endoplasmic reticulum stress in vascular cells: prevention by oxygen-regulated protein 150 expression. *Circ Res* 104: 328–336, 2009.
49. Seccia M, Albano E, and Bellomo G. Suitability of chemical *in vitro* models to investigate LDL oxidation: study with different initiating conditions in native and alpha-tocopherol-supplemented LDL. *Clin Chem* 43: 1436–1441, 1997.
50. Sies H. Oxidative stress: oxidants and antioxidants. *Exp Physiol* 82: 291–295, 1997.
51. Srinivasan S, Hatley ME, Reilly KB, Danziger EC, and Hedrick CC. Modulation of PPARalpha expression and inflammatory interleukin-6 production by chronic glucose increases monocyte/endothelial adhesion. *Arterioscler Thromb Vasc Biol* 24: 851–857, 2004.
52. Stadtman ER. Protein oxidation in aging and age-related diseases. *Ann N Y Acad Sci* 928: 22–38, 2001.
53. Steffen Y, Jung T, Klotz LO, Schewe T, Grune T, and Sies H. Protein modification elicited by oxidized low-density lipoprotein (LDL) in endothelial cells: protection by (-)-epicatechin. *Free Radic Biol Med* 42: 955–970, 2007.
54. Steinberg D. Low density lipoprotein oxidation and its pathobiological significance. *J Biol Chem* 272: 20963–20966, 1997.
55. Steinbrecher UP. Receptors for oxidized low density lipoprotein. *Biochim Biophys Acta* 1436: 279–298, 1999.
56. Tedgui A and Mallat Z. Cytokines in atherosclerosis: pathogenic and regulatory pathways. *Physiol Rev* 86: 515–581, 2006.
57. Traber MG and Atkinson J. Vitamin E, antioxidant and nothing more. *Free Radic Biol Med* 43: 4–15, 2007.
58. Uchida K, Kanematsu M, Morimitsu Y, Morimitsu Y, Osawa T, Noguchi N, and Niki E. Acrolein is a product of lipid peroxidation reaction. Formation of free acrolein and its conjugate with lysine residues in oxidized LDLs. *J Biol Chem* 273: 16058–16066, 1998.
59. Uchida K. Role of reactive aldehyde in cardiovascular diseases. *Free Radic Biol Med* 28: 1685–1696, 2000.
60. Ushio-Fukai M, Tang Y, Fukai T, Dikalov SI, Ma Y, Fujimoto M, Quinn MT, Pagano PJ, Johnson C, and Alexander RW. Novel role of $gp91^{phox}$-containing NAD(P)H oxidase in vascular endothelial growth factor–induced signaling and angiogenesis. *Circ Res* 91: 1160, 2002.
61. Vieira O, Escargueil-Blanc I, Jurgens G, Borner C, Almeida L, Salvayre R, and Nègre-Salvayre A. Oxidized LDLs alter the activity of the ubiquitin-proteasome pathway: potential role in oxidized LDL-induced apoptosis. *FASEB J* 14: 532–542, 2000.
62. Vindis C, Escargueil-Blanc I, Elbaz M, Marcheix B, Grazide MH, Uchida K, Salvayre R, and Nègre-Salvayre A. Desensitization of platelet-derived growth factor receptor-beta by oxidized lipids in vascular cells and atherosclerotic lesions: prevention by aldehyde scavengers. *Circ Res* 98: 785–792, 2006.
63. Willcox BJ, Curb JD, and Rodriguez BL. Antioxidants in cardiovascular health and disease: key lessons from epidemiologic studies. *Am J Cardiol* 101: 75D–86D, 2008.
64. Witztum JL and Steinberg D. Role of oxidized LDL in atherogenesis. *J Clin Invest* 88: 1785–1792, 1991.
65. Zadelaar S, Kleemann R, Verschuren L, de Vries-Van der Weij J, van der Hoorn J, Princen HM, and Kooistra T. Mouse models for atherosclerosis and pharmaceutical modifiers. *Arterioscler Thromb Vasc Biol* 27: 1706–1721, 2007.

Address correspondence to:
Dr. Anne Nègre-Salvayre
Biochimie
INSERM U858
CHU Rangueil
1 Avenue Jean Poulhès
BP84225
31432 Toulouse Cedex 4
France

E-mail: anne.negre-salvayre@inserm.fr

Date of first submission to ARS Central, May 21, 2010; date of final revised submission, October 19, 2010; date of acceptance, November 2, 2010.

Abbreviations Used

4-HNE = 4-hydroxynonenal
BV = bisvanilline
BVH = bisvanillyl-hydralazone
DHE = dihydroethidium
H_2DCFDA-AM = 6-carboxy-7′ dichlorodihydrofluorescein diacetate, di(acetoxymethyl ester)
HMEC-1 = human microvascular endothelial cell-1
IR = infrared
LDL = low-density lipoprotein
mp = melting points
OxLDL = oxidized LDL
PBS = phosphate-buffered saline
ROS = reactive oxygen species
SOD = superoxide dismutase
TBARS = thiobarbituric reactive substances

This article has been cited by:

1. Piotr Zimniak. 2011. Relationship of electrophilic stress to aging. *Free Radical Biology and Medicine* . [CrossRef]